

# **Hidden Time: Interpreting the geochemistry of Himalayan groundwaters**

Giovanni Bernardi

2024-2025

## **Abstract**

This is the abstract. Feel free to add anything insightful... or not :). Hello!

# **Contents**

<b>Abstract</b>	<b>i</b>
<b>1 Introduction</b>	<b>1</b>
1.1 Project Outline . . . . .	1
1.2 Lithological controls on weathering . . . . .	3
1.3 Dissolution rate findings . . . . .	3
1.4 Response to monsoonal precipitation . . . . .	3
1.5 Study aims . . . . .	4
<b>2 Study Area</b>	<b>5</b>
2.1 Geology and Geomorphic setting . . . . .	5
2.2 Climate and Vegetation . . . . .	5
2.3 The effect of the monsoon on the landscape . . . . .	5
<b>3 Data collection and analysis</b>	<b>7</b>
3.1 Field Sampling . . . . .	7
3.2 Major and Trace Element Analysis . . . . .	7
3.3 Sr Isotope Analysis . . . . .	7
3.4 Cyclic and hydrothermal Correction + radiogenic? . . . . .	7
<b>4 Results</b>	<b>9</b>
4.1 Springs changing concentration with season, indicating monsoonal precipitation influence . . . . .	9
4.2 Time series spring concentration changing over time . . . . .	10
4.3 Spatial concentration changes between the springs . . . . .	11
4.4 Sr isotope against $1/\text{Sr}$ data . . . . .	15
4.5 Traverse 3 is the best sampled and least influenced . . . . .	15
<b>5 Discussion</b>	<b>19</b>
5.1 Weathering Proxies from Strontium Isotopes . . . . .	19
5.2 Stoichiometric Considerations . . . . .	22

5.3	One-Dimensional Reactive Transport Model . . . . .	24
5.3.1	Fontorbe Model . . . . .	25
5.3.2	Maher Model . . . . .	29
5.3.3	Comparison of the Models . . . . .	33
5.3.4	Constraints on Residence Time . . . . .	34
5.4	Free Energy Calculations . . . . .	35
5.4.1	Comparison with Residence Time . . . . .	35
5.4.2	Constraints on Reaction Rate . . . . .	37
<b>6</b>	<b>Appendix 1: Dimensional Analysis of <math>T_f</math></b>	<b>40</b>

## **Acknowledgements**

Thanks Babe

## **List of Tables**

## **Nomenclature**

Add geology eg HHCS Silicate Weathering

All the variables

# 1 Introduction

## 1.1 Project Outline

Silicate weathering, whereby silicate minerals are dissolved by carbonic acid, sequesters atmospheric CO<sub>2</sub> over long (10<sup>5</sup> year) timescales, influencing global climate regulation. The Himalayan mountain range spans more than 590,000 km<sup>2</sup>, and is the source of major rivers, including the Ganges, Brahmaputra, and Indus.

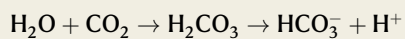
In highly erosive regions where the supply of silicate minerals far exceeds the weathering rate, silicate weathering reactions are thought to be sensitive to climate (Stallard & Edmund 1983 JGR, West et al, 2005) The dissolution kinetics of the largely silicate rocks in these catchments are sensitive to temperature and runoff because the weathering reactions have not gone to completion. Silicate weathering in the Himalayas as a result of their uplift and erosion in the Cenozoic may have contributed significantly to the global cooling over the past 40 million years (Raymo and Ruddiman, 1992; West et al, 2005, Kump et al, 2000 Ann Rev Earth Sci). Thus, it is this sensitivity to climate as well as their large size that makes them important to study, from both a scientific and practical perspective. More recent models have proposed silicate weathering is more sensitive to the hydrological cycle, than to temperature [cite]. There are a range of flow paths with different residence times, and rock is exhumed through these flow paths with a much longer time constant than the water in the flow paths.

However, there remain a number of unknowns in the weathering fingerprints of these catchments, namely the residence time of the water, flow path direction and length, rate of reaction, and extent to which equilibrium is reached. Understanding residence time in particular is important because the geochemical reactions that are used to quantify weathering (and the biogeochemical ones too) are time-dependent. Residence time will also reflect the variety of flow routes within a catchment, and help to constrain hydrological models. In this contribution the flow paths and residence times of water will be investigated using the chemical weathering products of spring waters from a highly monitored Himalayan catchment. This will not only provide better constraints on reaction rates of silicate mineral dissolution reactions in the field, but also a greater understanding of the role of hydrology in providing a climate-sensitive negative feedback between atmospheric CO<sub>2</sub> and silicate mineral dissolution An added benefit will also be provided via a greater understanding of Himalayan water supplies which are essential for billions of people (Ives and Messerli, 1989).

## Box 1

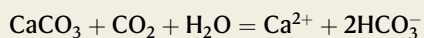
### Chemical Weathering

As water passes through the subsurface, it interacts with rock. This causes the addition of solute species to water, and the formation of stable secondary minerals through the dissolution of primary minerals formed at different pressure and temperature. Dissolved CO<sub>2</sub> derived from the atmosphere present in rainfall makes it slightly acidic. This acidity is further increased by the presence of decomposition of organic matter and CO<sub>2</sub> production from organic activity in the soil.



Carbonic Acid Weathering of Carbonate - Net Zero

Short Term [timescale]:

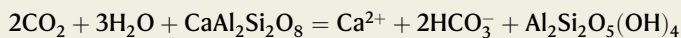


Long Term [timescale]:



Carbonic Acid Weathering of Silicate - Net CO<sub>2</sub> drawdown

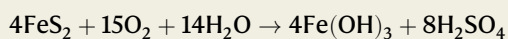
Short Term [timescale]:



Long Term [timescale]:



The rate of weathering is dependent on the mineralogy of the rock. Different minerals weather at different rates (from Shand et al, 1999: quartz > albite > mafic silicates > anorthite > carbonates), so the most reactive minerals will contribute disproportionately to the solute load of the water. [Something about Tipper 2006 and carbonates during monsoon?? somewhere]. Note that here, only the weathering of carbonic acid is considered. Sulfuric acid is also often considered a big player in weathering, but its impact is not considered in this study because the pyrite deposits required for its formation are not present in lithological studies of the Melamchi region [follow up].



Mineral reactions are also time-dependent, so the longer that water spends in contact with the rock, the higher the degree of completion of a chemical reaction [can mention incongruent dissolution whereby only part of the mineral dissolves?]. Current models of silicate and carbonate weathering (the two dominant lithologies considered) do not generally consider underground flow paths in their carbon flux estimates (Gaillardet et al, 1999 and others). Hence, a potentially underestimated part of the carbon cycle is this underground weathering.

## **1.2 Lithological controls on weathering**

Differences in lithology are thought to affect weathering. Geological differences lead to differences in soil composition, landscape features, vegetation, and climate which in turn affect the rates of reaction. Logically, the contribution of one lithology to weathering is correlated to its spatial extent in the catchment (Stallard and Edmond, 1983). Porosities vary widely across a catchment depending on the rock type encountered (Singh et al, 1987; David et al, 1994). Porosity also increases as a rock becomes more weathered (Marques et al, 2009). Weathering regimes can be classified as either transport-limited or kinetically limited (West et al., 2005). West et al. distinguish the two regimes by the rate of erosion in the catchment. In low erosion rate settings, weathering is transport-limited due to limited mineral supply. Weathering here is therefore proportional to the material eroded. In high erosion rate settings, weathering is kinetically limited due to an abundant mineral supply. Rapidly eroding catchments like Melamchi are therefore likely kinetically limited. Soil properties and topography are used to identify different "weathering regimes" in the subsurface (Pedrazas et al, 2021). Indeed, bedrock strength is thought to be more dependent on weathering than mineral or textural differences between the metamorphic lithologies in the Himalayas (Medwedeff et al, 2021).

## **1.3 Dissolution rate findings**

There is general consensus in the scientific community that rates of dissolution of minerals are different depending on whether they are measured in the field or in a laboratory. White and Brantley (2003) explain this difference by denoting 'extrinsic' qualities that are variable in the field, such as permeability and mineral/fluid ratios. The rate of dissolution of a mineral has also been linked to the free energy of the system, with laboratory rates being calculated significantly more far away from equilibrium (a higher delta G) than field rates (Kampman et al, 2009). This implies that field localities are closer to equilibrium than laboratory-derived rates might suggest. Add Maher et al, 2009 and why they think lab and field are different.

## **1.4 Response to monsoonal precipitation**

What makes the Himalayas unique is also what makes them difficult to model, namely the monsoon. This is characterised by a strong seasonal reversal of winds, which brings heavy rainfall to the region during the summer months, and dry conditions during the winter (Bookhagen and Burbank, 2010). The monsoon brings a large amount of precipitation to the region. Andermann et al. (2012) show that anticlockwise hysteresis loops of precipitation against discharge (include basic schematic) suggest that there is a 3 month lag in the response of the river to precipitation. The delay in river discharge is a topic of debate. Andermann et al. (2012) propose that at lower elevations,

it is more likely due to groundwater storage of precipitation in the fractured basement. Bookhagen and Burbank (2010) suggest that the delay of precipitation and discharge may be due to the response of glaciers at higher elevations. They also suggest evapotranspiration has a low impact on the hydrological budget of the Himalayas, less than 10%. Other studies have found that catchments with little glacial input show the same delay, suggesting that the former hypothesis may be more relevant to this discussion (McGuire et al, 2005). The residence time of groundwater can hence be used to quantify this delay and nature of its origin.

## 1.5 Study aims

In the present study, spring and rain samples from the Melamchi catchment are used as a case study to investigate the weathering rates in a rapidly eroding catchment. The sample dataset consists of 372 samples spanning four field campaigns over three years (2021-2024), as well as more recent year-long bi-weekly timeseries data from stream and spring samples in sites across the catchment. [See map] As Tipper et al, 2006 writes, studying small catchments gives the opportunity to attribute large changes in water chemistry to seasonal climate changes like the monsoon. (More in Area)

This study considers major and trace ion concentrations, alkalinity, and radiogenic strontium isotopes from the Melamchi catchment. This study shows that there are systematic variations in the chemical composition of the water along and away from the ridge. These can be explained through lithological differences and chemical weathering respectively. Estimation of the carbon flux in the groundwater yields \*\*\*\*\*?. Residence time calculations determined using rate constants close to equilibrium give ages of 10-25 years. This is in agreement with previous studies which calculated residence times using gas ages (Atwood et al [expand on this]). Previous studies have linked residence time to topography, such that areas with a small topographic gradient evolve to a larger residence time and vice versa. (McGuire et al, 2005). A similar relationship is found in this study.

So far, papers modelling the evolution of weathering have not considered catchment-based data due to the non-ideal setting. This study aims to bridge that gap by applying simplified models to a highly monitored catchment. The hope is that this approach will help to give a first-order estimation on parameters that are not easily obtained with the chemistry of a system alone. This report aims to join together studies looking at the same problem from different disciplines.

## **2 Study Area**

The Melamchi-Indrawati catchment (85.441 - 85.601E, 27.822 - 28.157 N) study area ranges from 790 to 5700 m a.s.l. (metres above sea level). The Melamchi River is a tributary of the larger Indrawati River and runs through the catchment draining an area of 325km<sup>2</sup>.

### **2.1 Geology and Geomorphic setting**

The geology of Melamchi is characterised by the characteristic banded gneiss, feldspathic schist and laminated quartzite of the Higher Himalayan Crystalline Sequence (HHCS). To the south of the confluence of the Melamchi River to its parent Indrawati river lies the Main Central Thrust (MCT) which separates the HHCS from the Lower Himalayan Sequence (LHS) (Dhital et al, Graf et al). The overall geology is therefore largely comprised of silicate metamorphic rock.

### **2.2 Climate and Vegetation**

There are two main climatic influences in the Himalayas: the monsoon system and the westerlies (Bookhagen and Burbank, 2010). The westerly winds typical of this latitude are responsible for the dry season in the Himalayas. The source of precipitation during the Indian Summer Monsoon (ISM) affecting Melamchi is the Bay of Bengal, due to the strong pressure gradient that changes the westerly winds to southerly winds. This is supported by isotopes... (Acharya et al, 2020). This temperature gradient reverses in the winter, when the oceans are warm and the High Himalaya is cold. The Melamchi Khola catchment receives over 80% of its rainfall during the monsoon. The seasonal variation in rainfall is thought to relate to different hydrological regimes, whereby river discharge and precipitation are 'coupled' when there is a significant enough amount of water to recharge the groundwater system. (Illien et al, 2021) The seasonal variation in precipitation therefore also translates to a variation in runoff, whereby this is twelve times stronger during the monsoon than during the dry season (Sharma, 1997).

### **2.3 The effect of the monsoon on the landscape**

During the monsoon, higher elevations receive more water from the southerly winds compared to the westerlies. Oxygen isotopes suggest most of the precipitation occurs in the higher elevation parts of the catchment (Acharya et al, 2020), though lapse rate has been used to suggest the foothill slopes receive the most amount of rain (Kattel et al, 2012). The southern Himalayas are characterised by a large topographic gradient. This corresponds to a large temperature gradient

contributing to tropical and alpine climates close to one another (Kattel et al, 2012). Changes in climate contribute to changes in the monsoonal system dynamics. The start of the monsoon has not changed in Nepal, but the end has been delayed. This has led to more intense precipitation on a per day basis, which is detrimental for crops in the winter season due to lack of moisture. Intense precipitation is also considered the main climatic cause of flooding (Panahi et al, 2015; Baniya et al, 2012).

Annual mean temperatures in the Melamchi Khola Catchment range from 24°C at base elevation to 8°C at highest elevation sampled (3200 m a.s.l.). The area is characterised by a high erosion rate. "One-off" landslide events transport as much as four times the flux of sediment deposited in the valley in a year (Chan Mao Chen et al, 2023). These events are thought to be increasing in frequency over recent years as a result of climate change, increasing the erosion rate in these areas (Adhikari et al, 2023). In particular, effects of a flash flood in 2021 are still visible in the area, with damage done to several bridges and hundreds of families. (insert picture of flooding)

<b>Catchment</b>	<b>Area</b>	<b>Mean</b>	<b>Mean El-</b>	<b>Elevation</b>	<b>NDVI</b>	<b>Geology</b>	<b>Location</b>
		<b>Slope</b>	<b>elevation</b>	<b>Range</b>	<b>during</b>	<b>Sampling</b>	<b>Range</b>
	(km <sup>2</sup> )	(%)	(m)	(m)			(DD)
Melamchi Khola	325	20	2400	786 - 5697		HHCS	85.441 - 85.601 E 27.822 - 28.157 N

Table 1: Catchment characteristics of the study area.

### **3 Data collection and analysis**

#### **3.1 Field Sampling**

Two types of water body were sampled in the field: springs and rain. Springs were sampled from the closest identified source in the study area, and rain was collected in a rain gauge. Both were measured in the field for temperature, pH and TDS on a Hanna Instruments HI-991300 and EX-TECH DO700. The field measurements were done at the source for the springs, and back at base for the rain before titrating, 24 hours within having been collected. Six aliquots were collected for each spring for anion, cation, titration, DIC, isotope and archive purposes respectively. Rain samples had a smaller yield and so only three aliquots were collected, for ion, isotope and archive purposes. Both water body types were filtered through a 0.2 m PES membrane in a filtration unit prior to bottling. Cation and archive samples were acidified with concentrated  $\text{HNO}_3$  to give a pH of  $\sim 2$ , keeping the cations in solution. Samples were titrated with a Hach digital titrator with 0.0625M HCl to calculate the alkalinity of the water following the Gran Method (Gran, 1952).

#### **3.2 Major and Trace Element Analysis**

Ion concentrations were measured in Cambridge once back from the field. Cation concentrations were determined using a Agilent Technologies 5100 Inductively-Coupled Plasma Optical Emission Spectrometer (ICP-OES) using a calibration line made from a Nepalese spring stock solution. Anion concentrations were determined using a Dionex ICS-5000 Ion Chromatograph against the Battle-02 standard calibration line. Associated uncertainties range between 5-10% for cations and 10-15% for anions.

#### **3.3 Sr Isotope Analysis**

Samples were dried down to provide at least  $1 \mu\text{g}$  of Sr. Samples were then dissolved in aqua regia (3:1  $\text{HNO}_3:\text{HCl}$ ) to remove any additional organic matter. Once dried down again, they were added to  $30 \mu\text{l}$  teflon columns with Eichrom SrSpec<sup>®</sup> resin pipetted in. Once washing the column three times with Milli-Q<sup>®</sup> water, it was primed with 3N  $\text{HNO}_3$ . The sample was centrifuged then loaded onto the column avoiding any solids. The column was then washed a total of three times with 3N  $\text{HNO}_3$  to remove cations. Lastly the column was eluted to a beaker with Milli-Q<sup>®</sup> water to collect the Sr. Once dried, the samples were ...

#### **3.4 Cyclic and hydrothermal Correction + radiogenic?**

Rain input is a significant factor in the chemical composition of rivers (Drever, 1997). Spring water is corrected for rain input according to the average concentration for the closest rain sample

collected in this field season.

To remove the contribution of the rain the following formula is used for any element X:

$$[X]_{rain-corrected} = [X]_{river} \cdot (Cl_{river} - Cl_{river}^*) \frac{[X]_{rain}}{[Cl]_{rain}}$$

Where  $[Cl]_{river}^*$  is calculated by subtracting the concentration of chloride in the rain from that in the river (Tipper et al, 2006).  $Cl^*$  is taken to be zero if the concentration of chloride in the rain is greater than concentration of river. Evapotranspiration is not considered by this model, because of studies like Andermann et al (2012) which show that it plays a minor role, accounting for less than 10% of the hydrological budget in the Himalayas. They agree with Bookhagen and Burbank

In those cases where  $Cl^*$  is not zero then, a primary rain correction is simply:

$$[X]_{rain-corrected} = [X]_{river} - [X]_{rain}$$

Once the samples have been corrected for rain input, the remaining  $[Cl]^-$  is assumed to be derived from evaporites encountered in the flow path.

Hence, the sample with the highest  $[Cl]^-$  is used to correct the ions in a similar fashion to how the most dilute sample was used above:

$$[X]_{evaporite-corrected} = [X]_{rain-corrected} - \frac{[X]}{[Cl]_{highest-Cl}} * [Cl]_{rain-corrected}$$

This ensures that all chloride in the corrected sample is removed. The correction uses ionic ratios from the most concentrated water source, which acts as a proxy for the sediment imparting its signature. In this way, the correction does not affect samples which do not have high Cl (and hence do not have a large evaporite contribution), but does decrease the concentration of ions for those that do.

## 4 Results

### 4.1 Springs changing concentration with season, indicating monsoonal precipitation influence

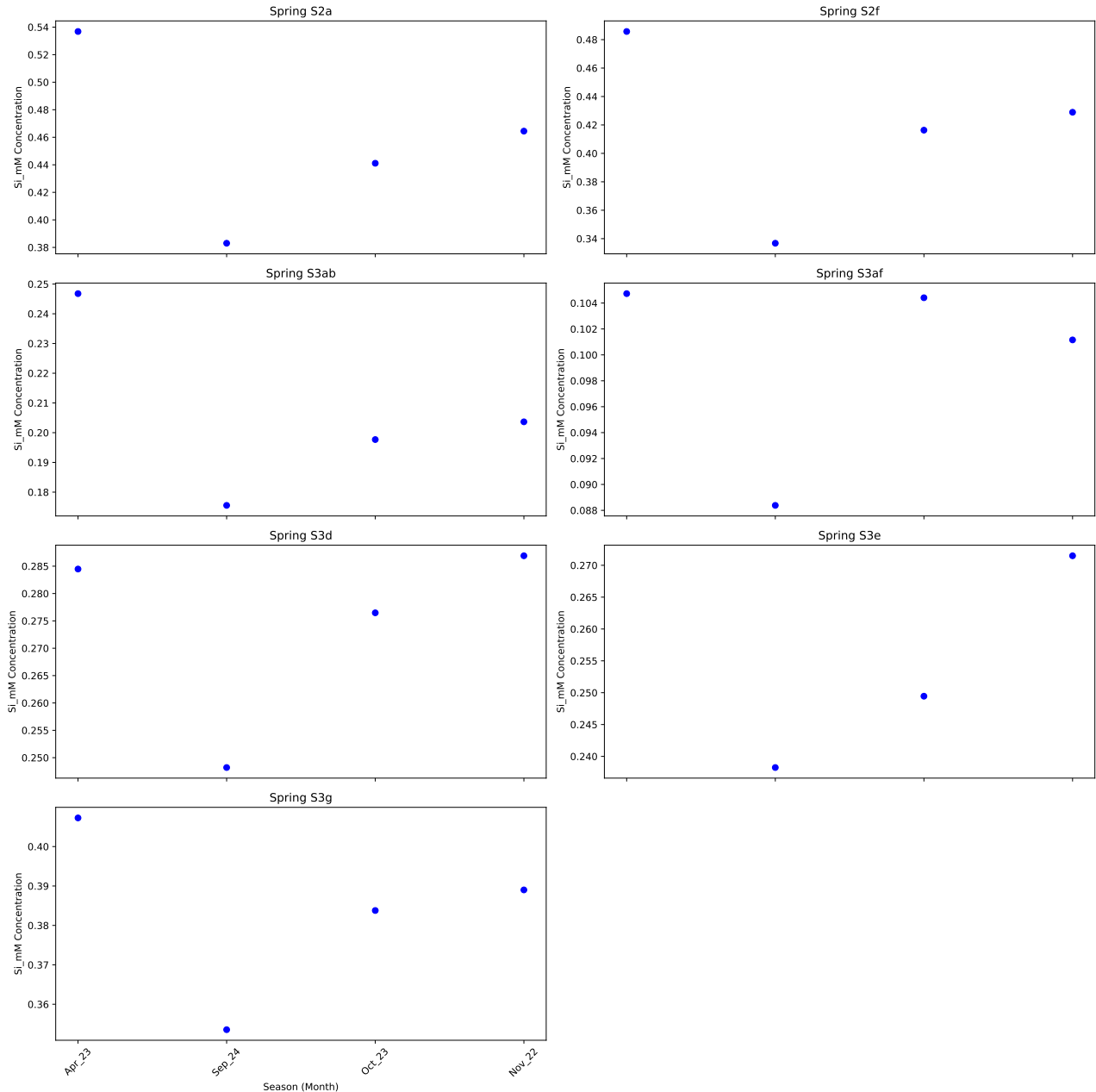


Figure 1: Seasonal changes in spring concentration indicating monsoonal precipitation influence.

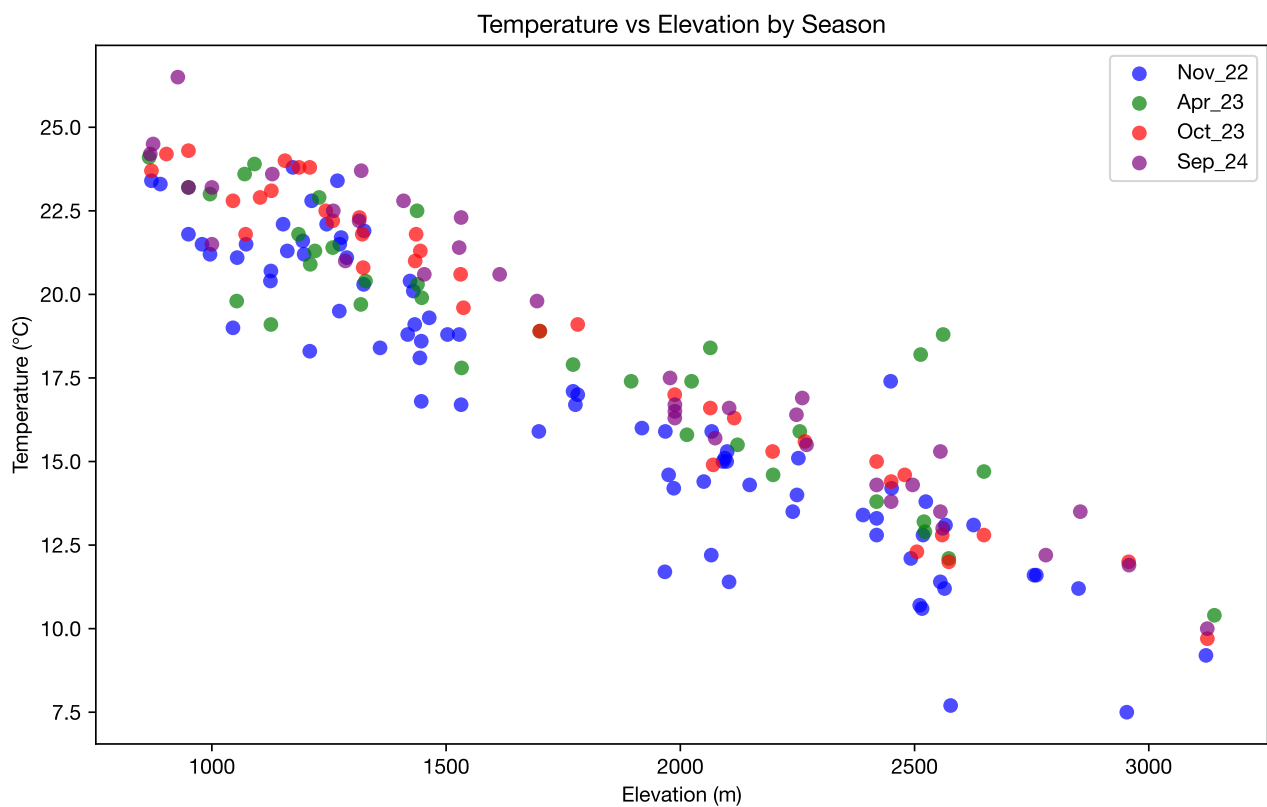


Figure 2: Temperature changes

## 4.2 Time series spring concentration changing over time

Concentration increases then decreases with monsoon.

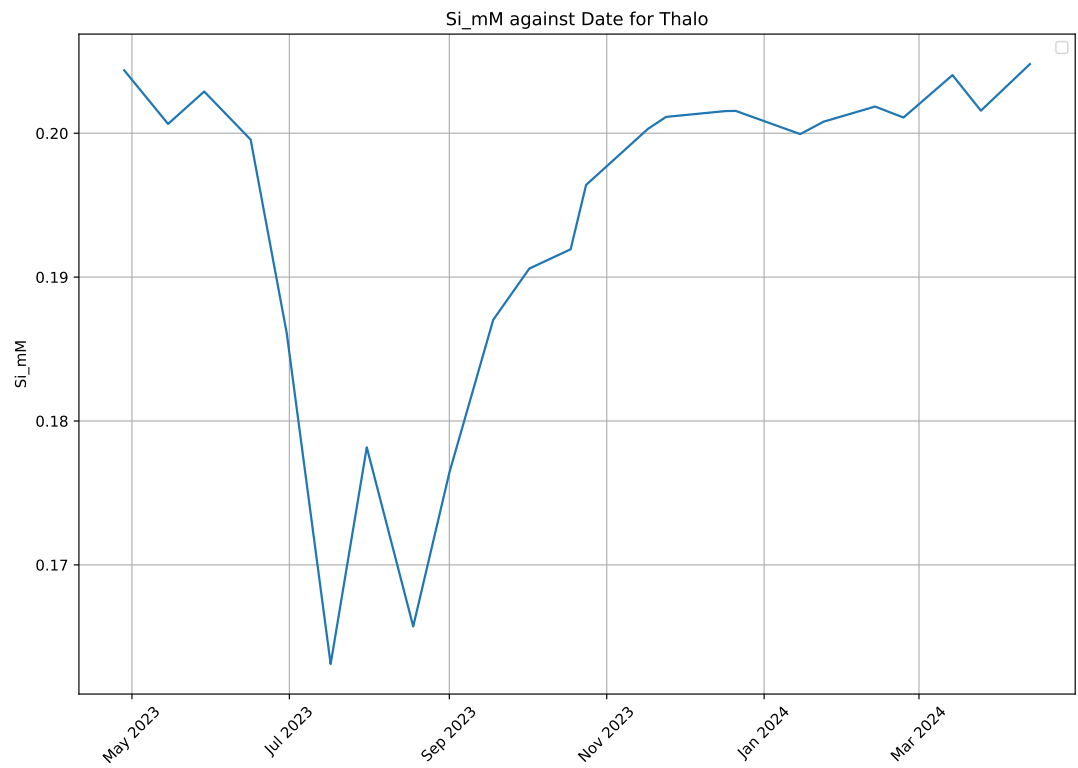
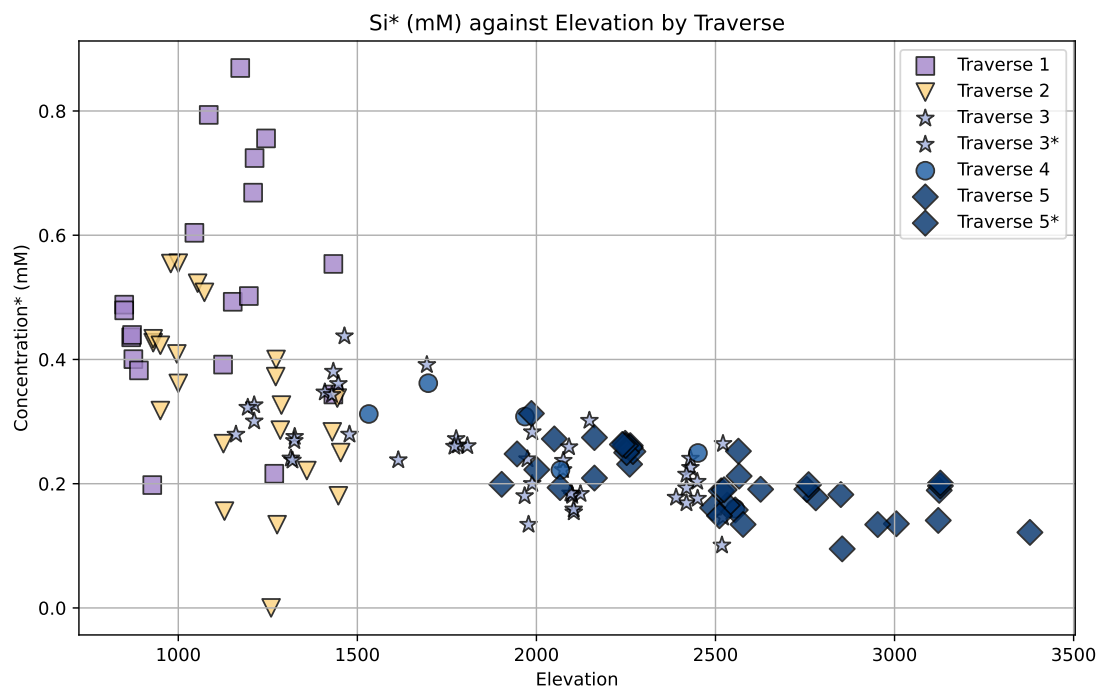
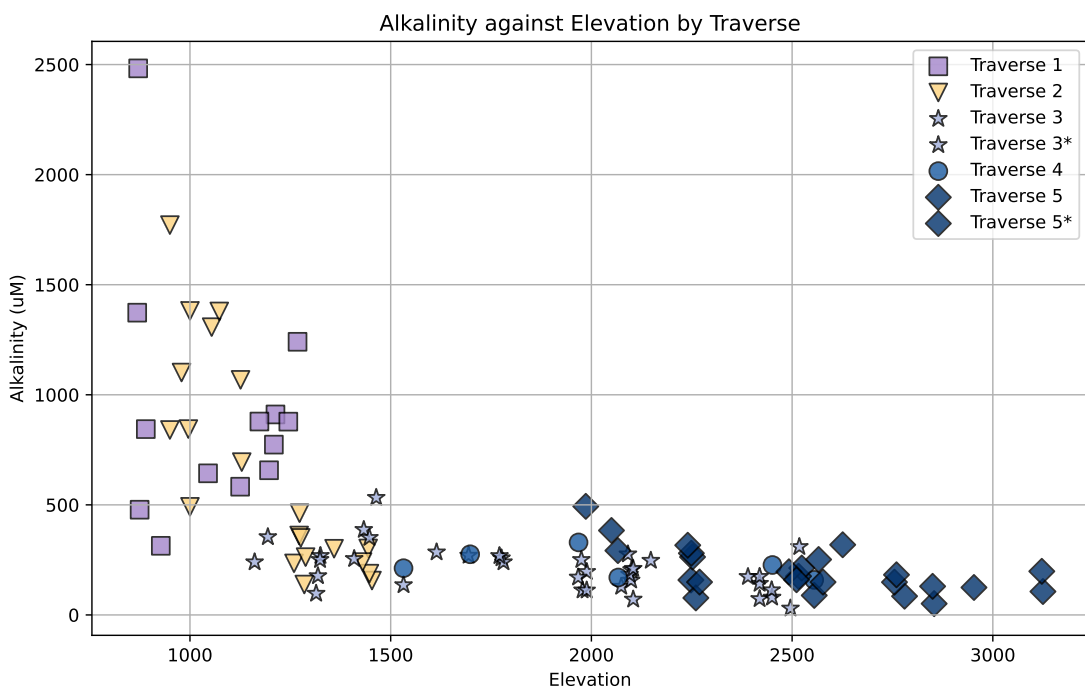


Figure 3: Time series of spring concentration changes over time.

### 4.3 Spatial concentration changes between the springs



**Figure 4: How Si changes with elevation**



**Figure 5: How Alkalinity changes with elevation**

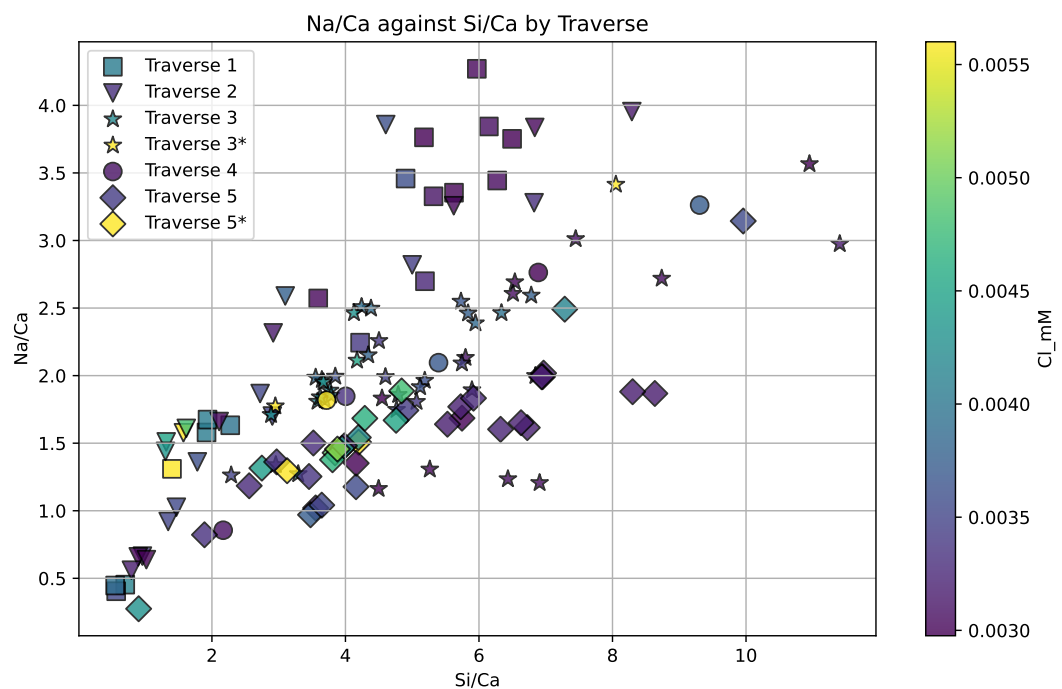


Figure 6: Si/Ca against Na/Ca. Clear differences between traverses.

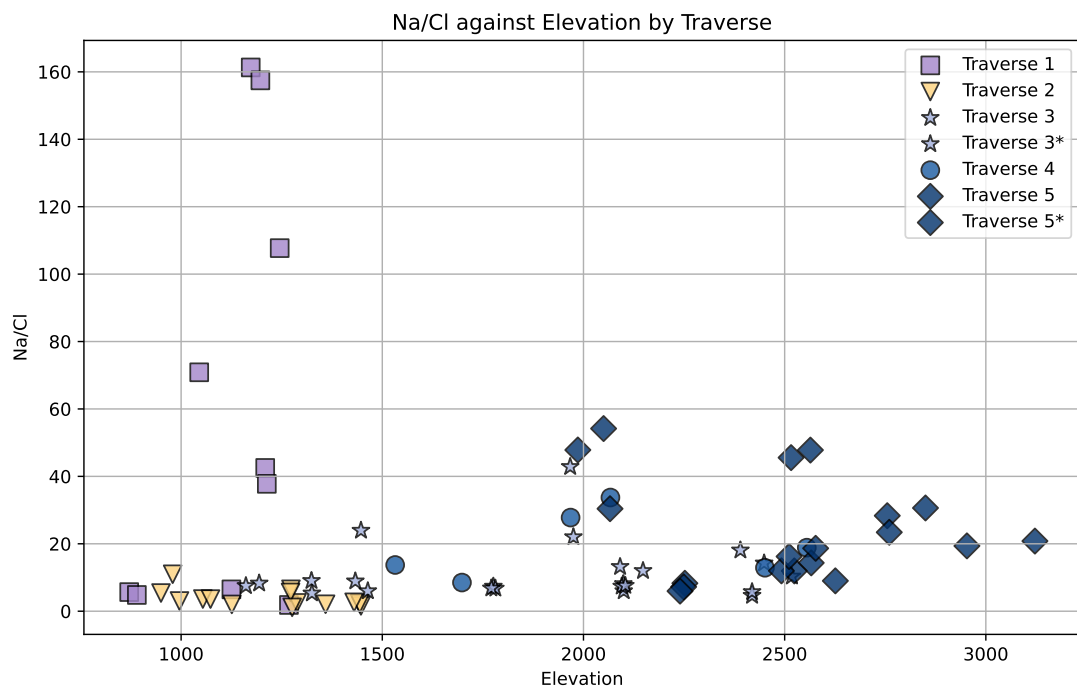


Figure 7: NaCl against elevation coloured by traverse - super low Cl

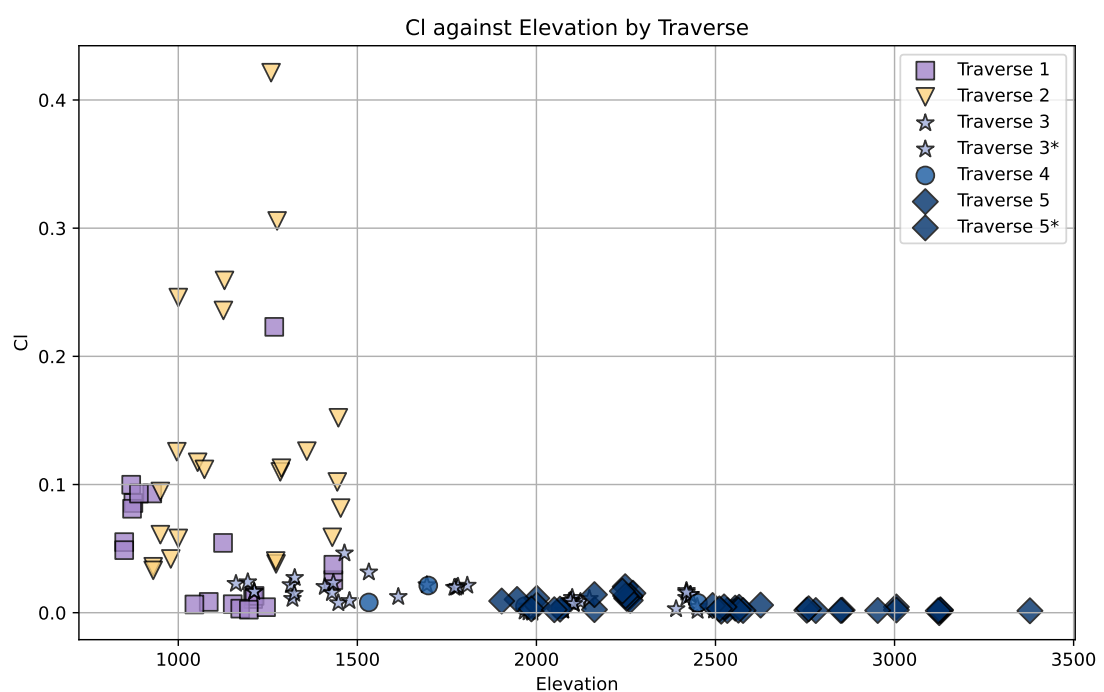


Figure 8: Cl against elevation coloured by traverse - Potential evaporite influence on traverse 2 water chemistry

#### 4.4 Sr isotope against 1/Sr data

To eliminate evaporation, shows the differences between the springs.

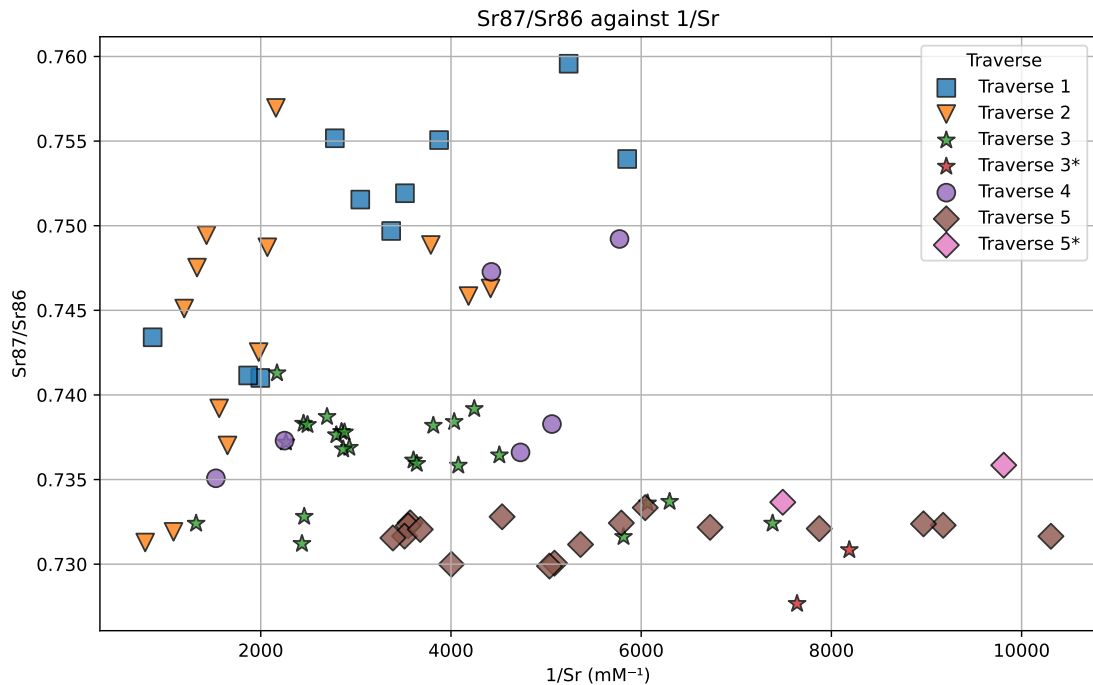


Figure 9: Strontium isotope differences display difference in lithology tapped in. Cite Quade and Tipper papers

#### 4.5 Traverse 3 is the best sampled and least influenced

This will be modelled.

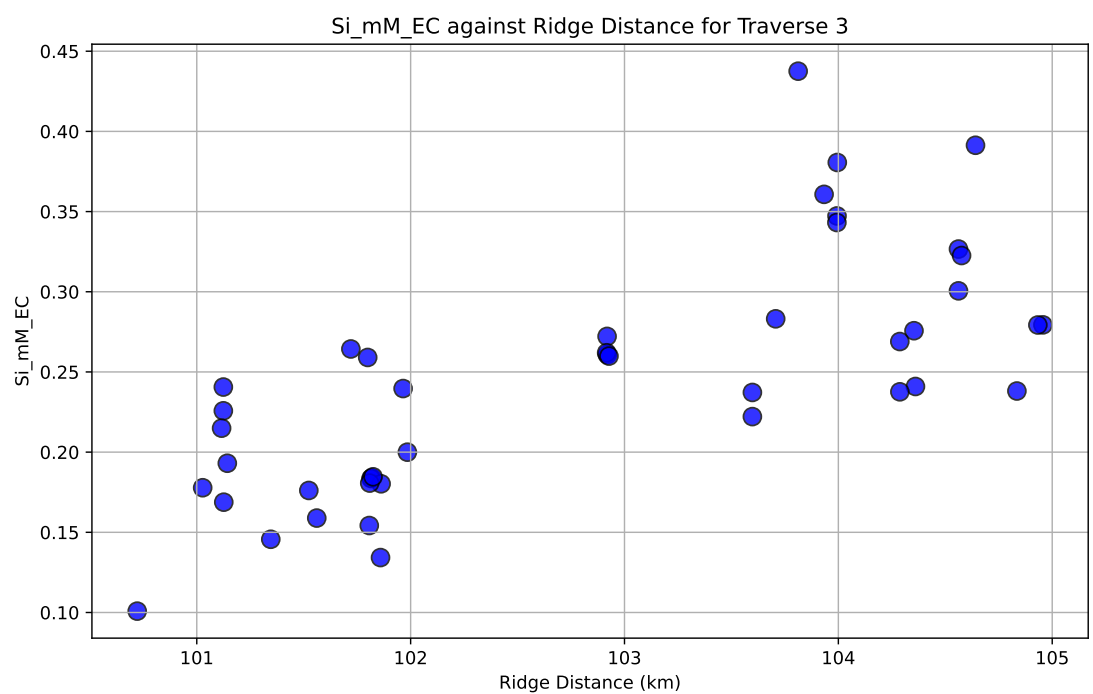


Figure 10: How Si varies for Traverse 3, and showing the wide variety of samples

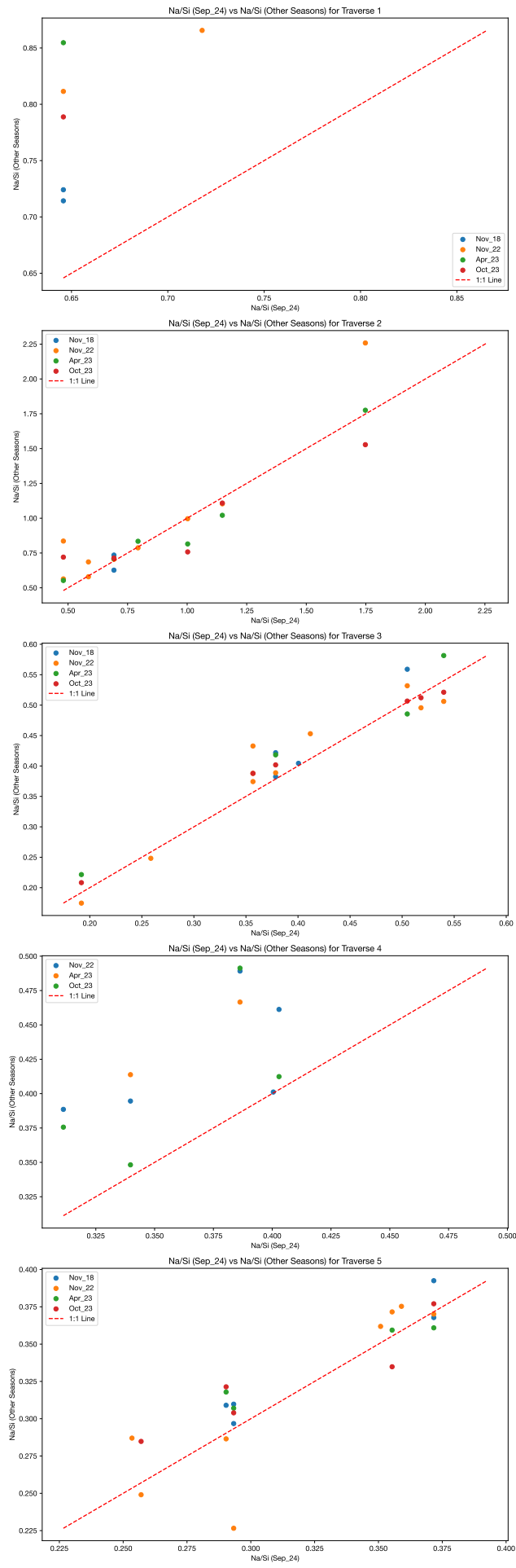


Figure 11: Na/Si for all traverses, Traverse 3 is pretty neat  
17

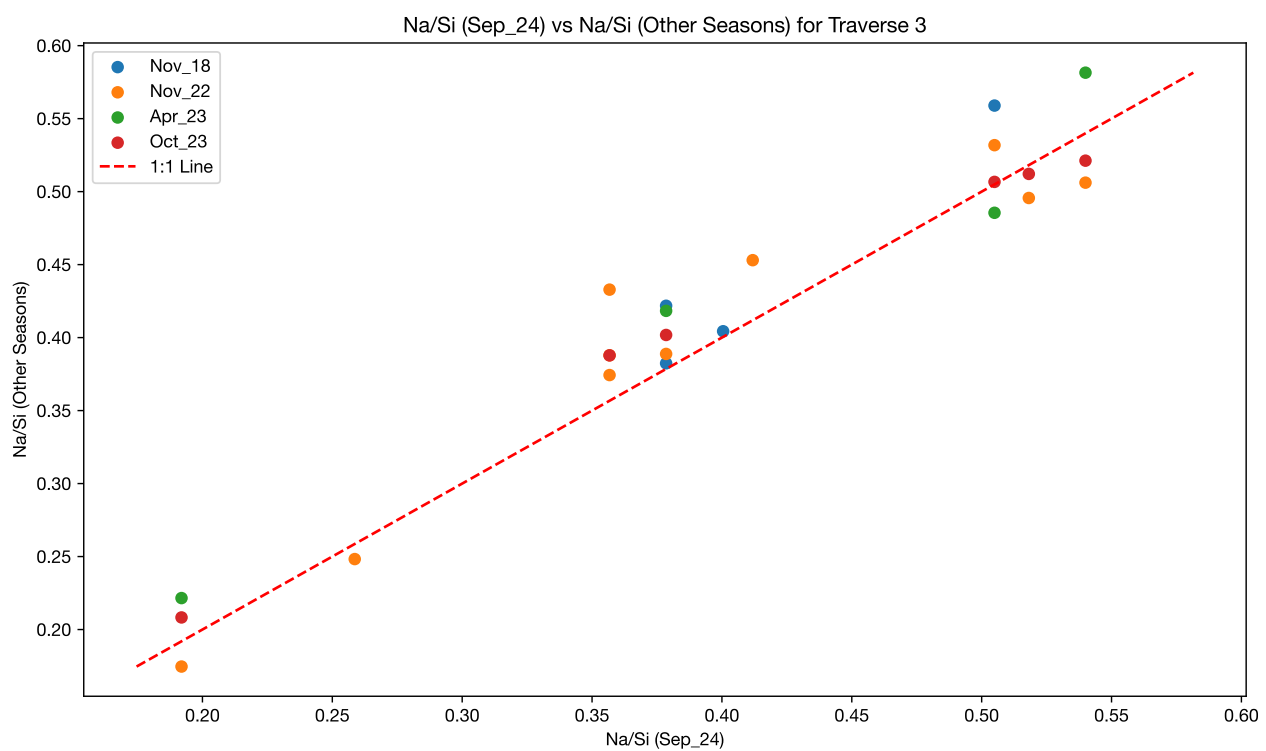


Figure 12: Na/Si for Traverse 3 is pretty neat

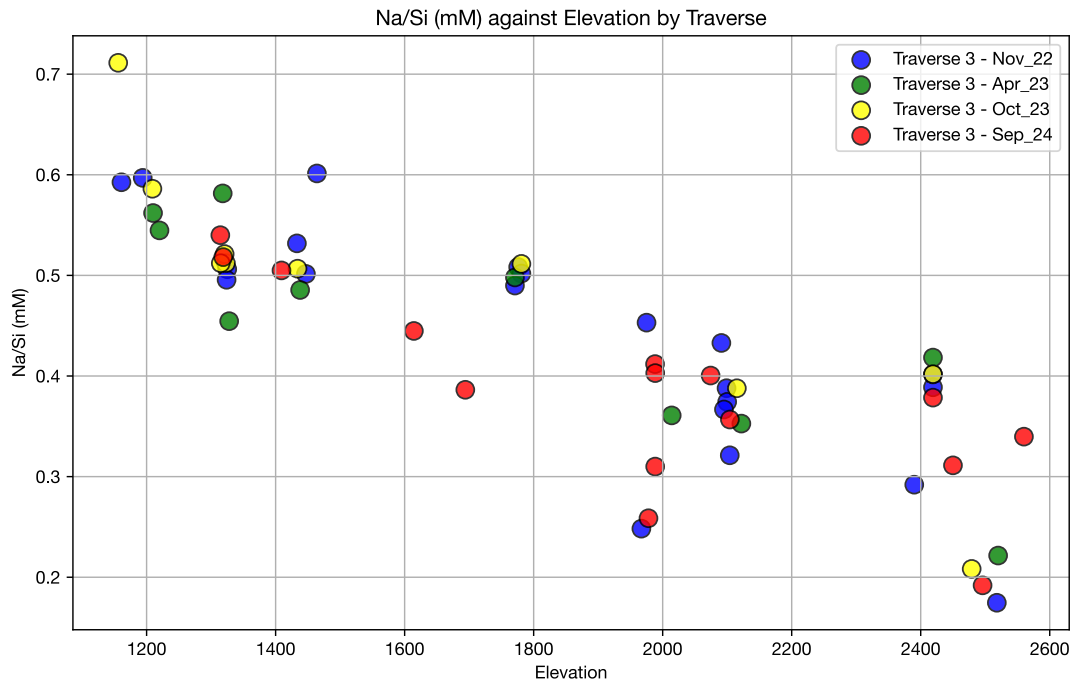


Figure 13: Na/Si for Traverse 3 is pretty neat. Consistently sampled flow paths

## 5 Discussion

### 5.1 Weathering Proxies from Strontium Isotopes

- Rain contribution suggests not much dust gets there at high elevations. Where is the cloud cover here?
- Sr against 1/Sr plot, suggesting springs are sampling different things with distance from the source. after Galy, France Lanord and Derry

Sr isotopes derived from the most recent rain analyses are of the order of 0.70904 to 0.70925 at the lowest. Seawater is of the order of 0.70917. Within error, therefore, the lowest rain values reflect seawater values, indicating little contamination from dust or particles. These are indeed found at the higher elevations

Also recreate the plot from Galy, France Lanord and Derry 1998

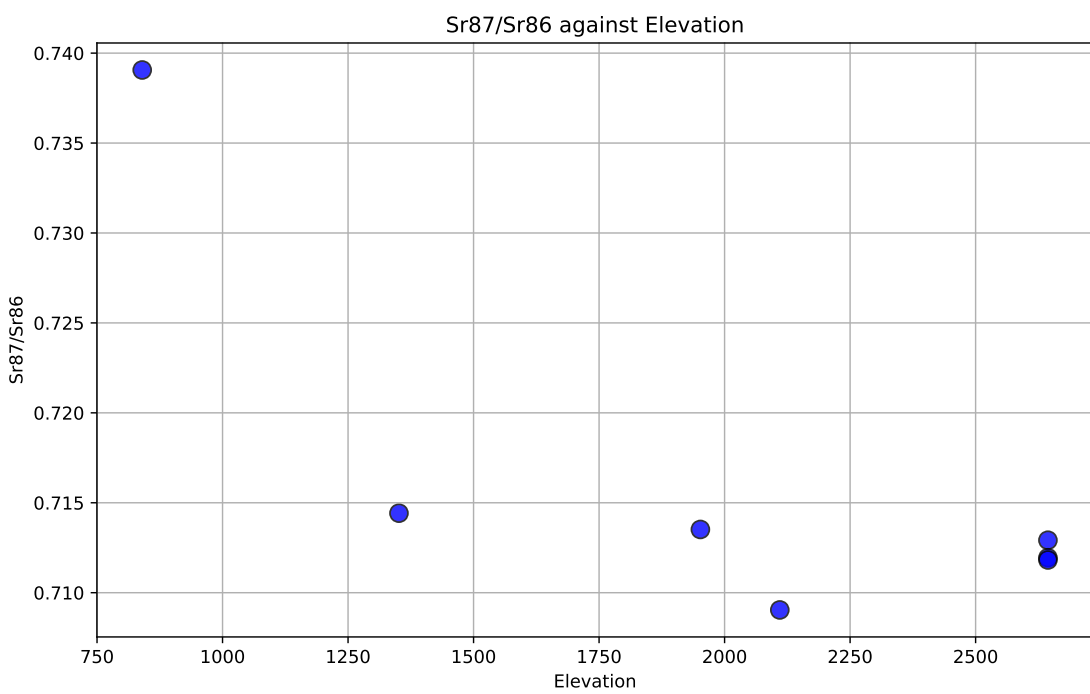


Figure 14: Rain analysed for Sr isotopes. Something about contamination lower down

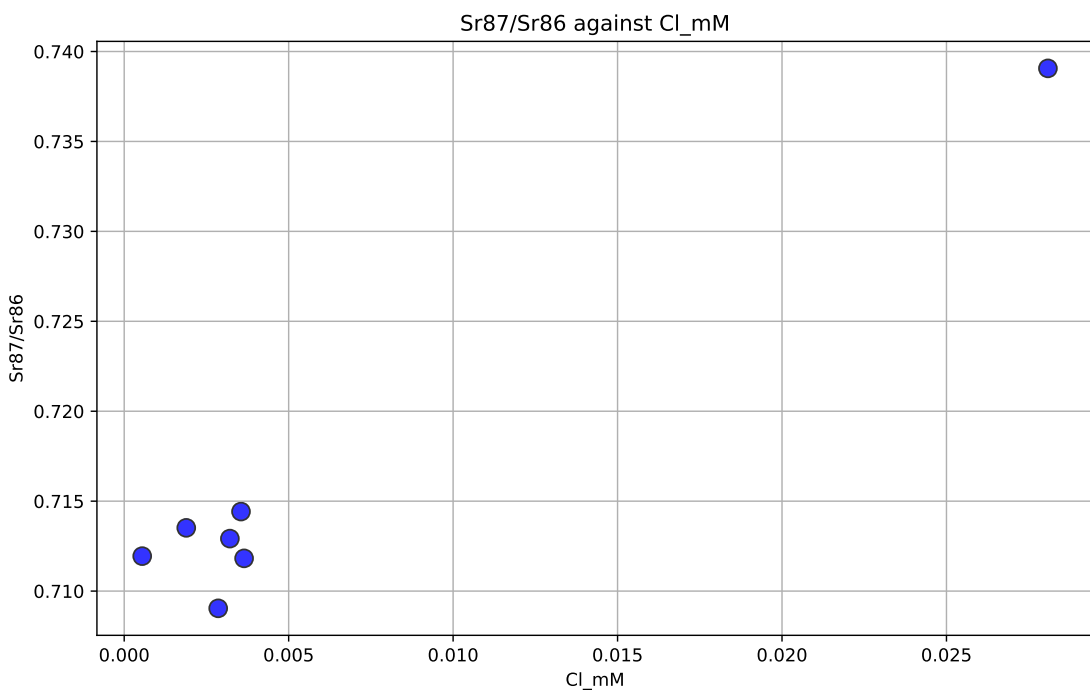


Figure 15: Rain analysed for Sr isotopes and Cl. Something about contamination lower down

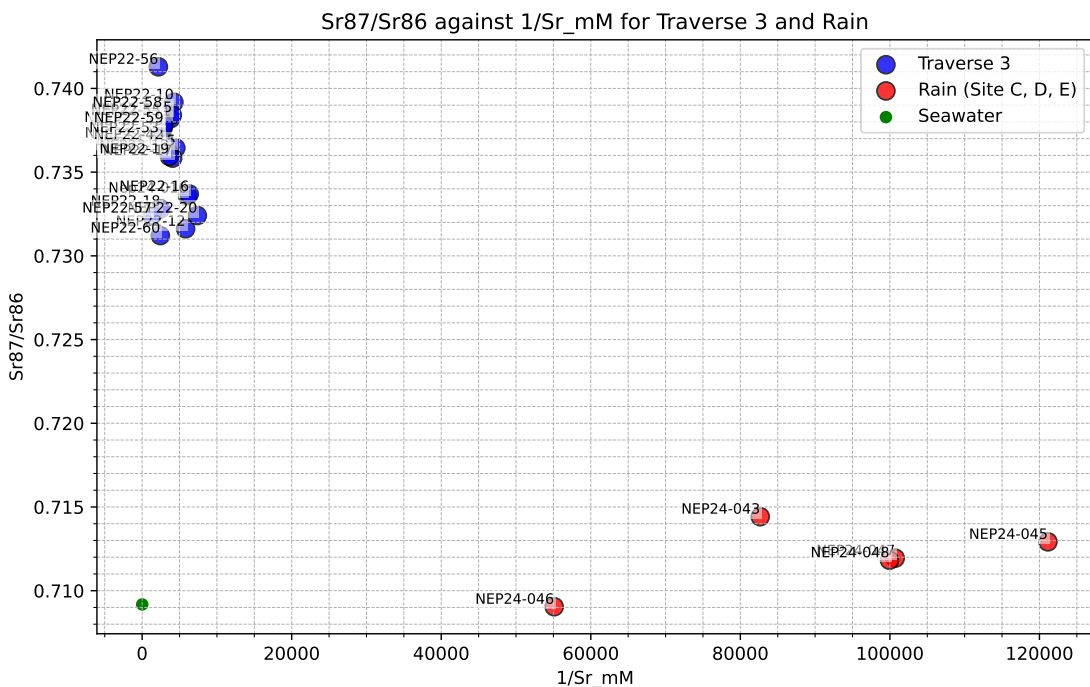


Figure 16: How samples of Traverse 3 compare to the rain samples

Also include 87Sr/86Sr weathering according to that mass balance thing... if that helps

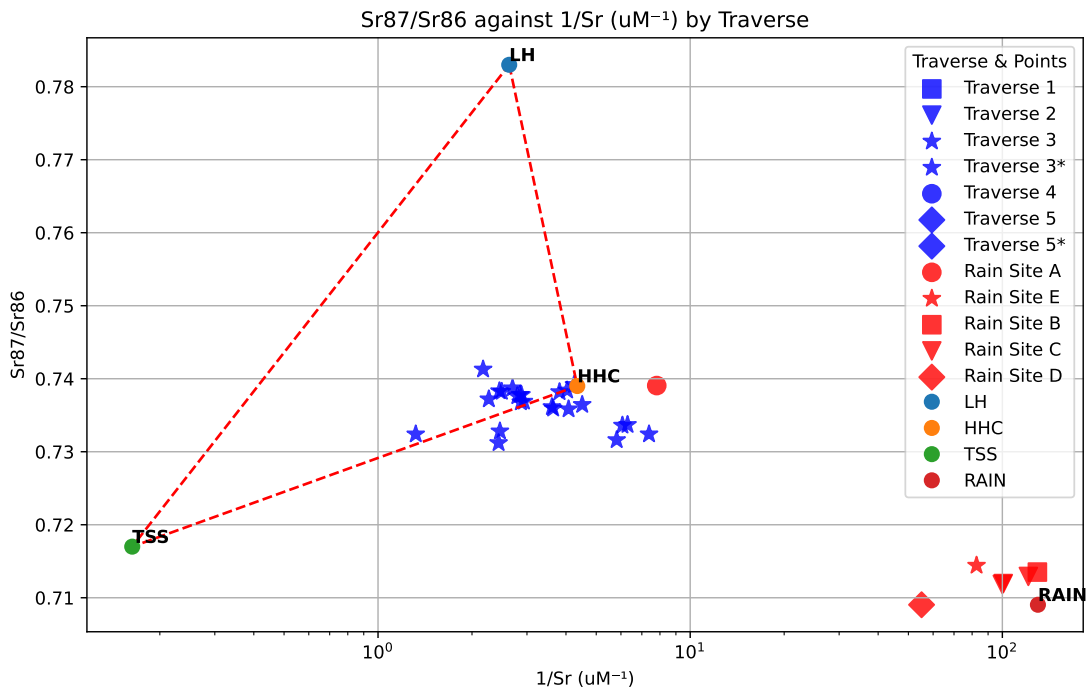


Figure 17: Recreating the Lanord plot etc. Need to choose better endmembers

## 5.2 Stoichiometric Considerations

- Matrix example
- Feldspar is mostly what we dissolve and kaolinite is mostly what we precipitate
- Include the stoichiometry of the reaction from Drever
- Decide that at Alakmanda, eg albite component is near 0.8

$$\begin{array}{ccccccccc}
 & Biot & Plag & cc & Smec & Kaol & 2nd cc & \mu\text{mol/l} & \text{River} \\
 Si & 2.58 & 2.76 & 0 & 3.55 & 2 & 0 & n_{Biot} & 44 \\
 Al & 2.37 & 1.24 & 0 & 1.88 & 2 & 0 & n_{plag} & 0 \\
 Mg & 0.84 & 0 & 0.053 & 0.37 & 0 & 0.013 & n_{cc} & 481 \\
 Ca & 0.01 & 0.245 & 0.944 & 0.1 & 0 & 0.987 & n_{smec} & 914 \\
 Na & 0.04 & 0.754 & 0 & 0.01 & 0 & 0 & n_{kaol} & 113 \\
 K & 0.67 & 0.006 & 0 & 0.16 & 0.01 & 0 & n_{2nd cc} & 29
 \end{array} = \begin{pmatrix} 44 \\ 0 \\ 481 \\ 914 \\ 113 \\ 29 \end{pmatrix}$$

A far more practical way is to make use of matrix algebra. If:

$$AX = B \quad (3)$$

where A and B are known matrices, but X is a matrix to be determined, then it follows that:

$$X = A^{-1}B \quad (4)$$

where  $A^{-1}$  is the inverse of of matrix A.

**Figure 18: Matrix example of what you need to write**

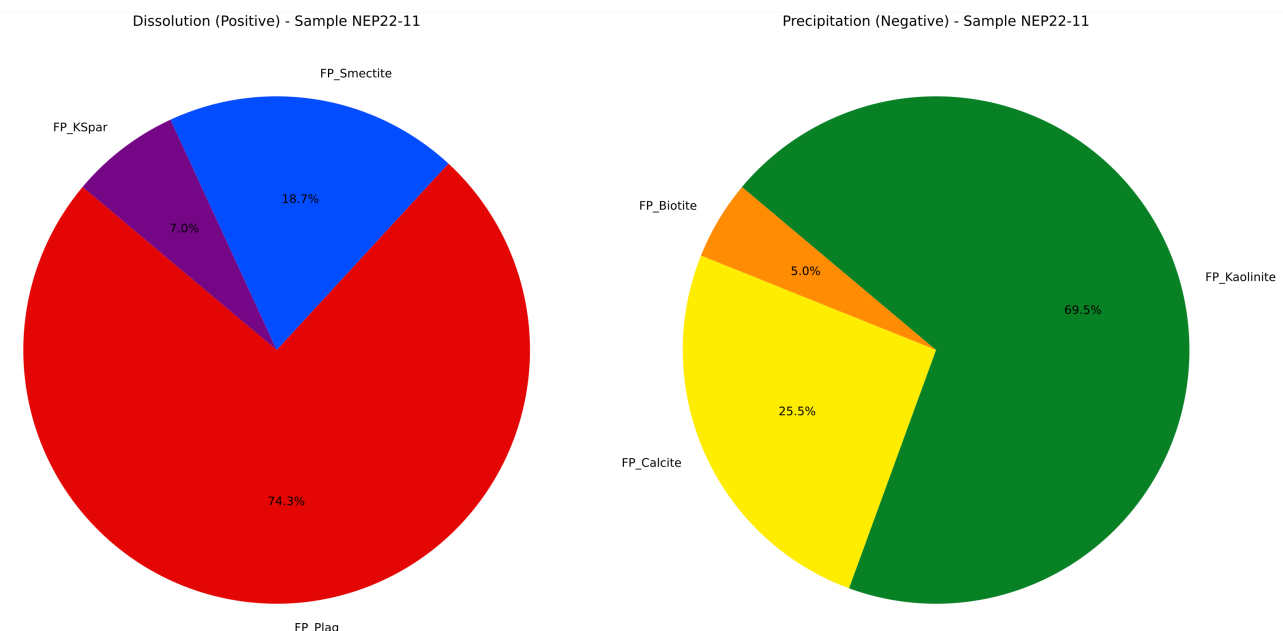


**Figure 19: Example dissolution plot**

### 5.3 One-Dimensional Reactive Transport Model

Need to talk about what previous papers have said and how our d<sub>18</sub>O predicts a particular flow path length eg.

Also need to make a mini 1D graphic explaining what the 1D model actually means in practice

- Explain the basis behind the model. Maher in that weathering is sensitive to fluid flux more so than it is to the temperature. Another interpretation is that of Fontorbe where it is sensitive to the temperature.
- From same first order differential equation we get two different models
- The Maher model because of less constraints the opposite can be used to calculate times for a given rate of reaction, and compare to Abra's already determined ages
- For Fontorbe we have a series of assumptions that allow us to calculate the rate of reaction which will allow us to determine whether we are close to eqm or not.
- The Maher model can also be used to determine the rate of reaction for a given set of concentrations and times
- Emphasise how the Maher model wants to predict what weathering is sensitive to

### 5.3.1 Fontorbe Model

Put the models in boxes?

Starts with a first order differential equation describing the reactive transport of Si, assuming reaction rates remain constant along the flow path, which is different from Maher.

$$\phi \frac{\partial C}{\partial t} = -\omega \phi \frac{\partial C}{\partial z} + R_n \cdot (1 - f) \quad (1)$$

Where C is Si concentration,  $\phi$  is porosity,  $\omega$  is the fluid velocity, z is the distance along the 1D flow path,  $R_n$  is the rate of reaction, and f is the fraction of Si reprecipitated in clay minerals. This value is just a function of much Si in the water is precipitated or dissolved.

We can then non-dimensionalise,  $z = hz'$  where h is the length of the flow path;  $t = ht'/w$ ,  $C = CoC'$  where  $Co$  is the initial Si concentration (but can be something else)

$$C' = \frac{C}{C_o} \quad \& \quad z' = \frac{z}{h} \quad \& \quad t' = \frac{t\omega}{h} \quad (2)$$

This transforms the equation 1 to:

$$\frac{\partial C'}{\partial t'} = -\frac{\partial C'}{\partial z'} + N_D \cdot (1 - f) \quad (3)$$

Where

$$N_D = \frac{R_n \cdot h}{\phi \cdot Co \cdot \omega} \quad (4)$$

Given a quasi-stationary state assumption (Lichtner, 1988), where  $\frac{\partial C'}{\partial t'} = 0$ , we can solve for the rate of reaction

$$C' = 1 + z' \cdot N_D \cdot (1 - f) \quad (5)$$

So when  $z = h$ , and  $z' = 1$ ,

$$N_D = \frac{C'_h - 1}{1 - f} \quad (6)$$

Where  $C'$  is the concentration of Si at the end of the flow path.

We also know that the residence time  $T_f$  is

$$T_f = \frac{h}{\omega} \quad (7)$$

So at the end of the flow path  $h$  for a concentration  $C'_h$ :

$$\frac{R_n \cdot h}{\phi \cdot Co \cdot \omega} = \frac{C'_h - 1}{1 - f} \quad (8)$$

$$\frac{R_n \cdot T_f}{\phi \cdot Co} = \frac{C'_h - 1}{1 - f} \quad (9)$$

$$T_f = \frac{(C'_h - 1) \cdot \phi \cdot Co}{(1 - f) \cdot R_n} \quad (10)$$

This can be rearranged for the rate of reaction,  $R_c$ . It can also be rearranged for time. We get:

$$C'_h = C_h/C_o \quad (11)$$

$$T_f = \frac{(C_h - C_o) \cdot \phi}{(1 - f) \cdot R_n} \quad (12)$$

Note that this equation leads to times coming out in  $10^{-9}$ s, so this needs to be accounted for when converting to years.

or

$$R_n = \frac{(C_h - C_o) \cdot \phi}{(1 - f) \cdot T_f} \quad (13)$$

Fontorbe			
Parameter	Definition	Units	Formula (Value)
$\phi$	Porosity	-	-
$\omega$	Fluid velocity	m/s	-
$h$	Length of flow path	m	Variable
$C_h$	Concentration end of flow path	$\mu\text{mol/L}$	Variable
$C_0$	Initial concentration	$\mu\text{mol/L}$	Rain Conc
$f$	Fraction reprecipitated	-	Order 0.5
$N_D$	Non-dimensional number	-	$N_D = \frac{R_n h}{\phi C_0 \omega}$
$T_f$	Residence time	$10^{-9} \text{ s}$	$T_f = \frac{h}{\omega}$
$R_n$	Reaction rate	$\text{mol/m}^3/\text{s}$	$k \cdot S \cdot \rho \cdot 10^3 \cdot X \cdot (1 - \phi)$
$k$	Reaction rate constant	$\text{mol/m}^2/\text{s}$	-
$S$	Specific surface area	$\text{m}^2/\text{g}$	-
$\rho$	Mineral density	$\text{kg/m}^3$	
$X$	Volume fraction of mineral in rock	$g_{min}/g_{rock}$	0.2

Table 2: Key parameters and definitions for the Fontorbe model.

### 5.3.2 Maher Model

The first order differential equation to solve is:

$$\frac{dc}{dt} = -\frac{q}{\phi} \frac{dc}{dx} + \sum_i \mu_i R_{d,i} \left( 1 - \left( \frac{c}{c_{\text{eq}}} \right)^{n_i} \right)^{m_i} - \sum_i \mu_i R_{p,i} \left( 1 - \left( \frac{c}{c_{\text{eq}}} \right)^{n_i} \right)^{m_i} \quad (14)$$

Where  $c$  is the concentration,  $q$  is the fluid flux,  $\phi$  is the porosity

Under the quasi-steady state assumption, we can write:

$$\frac{dc}{dx} = \frac{q}{\phi} \sum_i \mu_i R_{d,i} \left( 1 - \left( \frac{c}{c_{\text{eq}}} \right)^{n_i} \right)^{m_i} - \frac{q}{\phi} \sum_i \mu_i R_{p,i} \left( 1 - \left( \frac{c}{c_{\text{eq}}} \right)^{n_i} \right)^{m_i} \quad (15)$$

With

$$R_n = \sum_i \mu_i R_{d,i} - \sum_i \mu_i R_{p,i} \quad (16)$$

Given the definition of  $R_n$  as

$$R_n = \sum_i \mu_i R_{d,i} - \sum_i \mu_i R_{p,i} \quad (17)$$

Maher and Chamberlain describe that the reaction rate decreases linearly with approach to equilibrium.

$$\frac{dc}{dt} = R_n \left( 1 - \frac{c}{c_{\text{eq}}} \right) \quad (18)$$

Equation 15 can be solved for  $c$ , to obtain (following Maher and Chamberlain, 2013)

$$c(x) = c_0 \exp\left(-\frac{R_n \phi x}{qc_{\text{eq}}}\right) + c_{\text{eq}} \left(1 - \exp\left(-\frac{R_n \phi x}{qc_{\text{eq}}}\right)\right) \quad (19)$$

We also know that the residence time  $T_f$  is

$$T_f = \frac{L\phi}{q} \quad (20)$$

So

$$c(T_f) = c_0 \exp\left(-\frac{R_n T_f}{c_{\text{eq}}}\right) + c_{\text{eq}} \left(1 - \exp\left(-\frac{R_n T_f}{c_{\text{eq}}}\right)\right) \quad (21)$$

Following Maher and Chamberlain, 2014, this can be solved and rewritten:

$$C = \frac{C_0}{1 + \tau D_w / q} + C_{\text{eq}} \frac{\tau D_w / q}{1 + \tau D_w / q} \quad (22)$$

Where

$$\tau = e^2; \quad D_w = \frac{L\phi R_n}{C_{\text{eq}}} \quad (23)$$

This can therefore be rewritten as:

$$C = \frac{C_0 + C_{\text{eq}} \cdot T_f (e^2 \cdot R_n / C_{\text{eq}})}{1 + T_f (e^2 \cdot R_n / C_{\text{eq}})} \quad (24)$$

The equation can be rearranged for the residence time,  $T_f$ , which can be compared to the ages obtained from the Fontorbe model. We get:

$$T_f = \frac{C_{eq} \cdot (C - C_0)}{e^2 R_n (C_{eq} - C)} \quad (25)$$

Note that this equation leads to times coming out in  $10^{-6}$ s, so this needs to be accounted for when converting to years

or:

$$R_n = \frac{C_{eq} \cdot (C - C_0)}{e^2 T_f (C_{eq} - C)} \quad (26)$$

Maher			
Parameter	Definition	Units	Formula (Value)
$L$	Length of flow path	m	Variable
$q$	Flow rate	m/s	Variable
$\phi$	Porosity	-	0.3 (but variable)
$R_n$	Net reaction rate	mol/L/s	$\rho_{sf} \cdot k \cdot A \cdot X_r$
$\rho_{sf}$	Mass mineral / Fluid Volume ratio	g/L	$1000 \cdot \rho_b / \phi$
$\rho_b$	Plagioclase density	g/cm <sup>3</sup>	-
$k$	Reaction rate constant	mol/m <sup>2</sup> /s	-
$A$	Specific surface area	m <sup>2</sup> /g	0.1-1
$X_r$	Mineral concentration in fresh rock	$g_{min}/g_{rock}$	Wt% in rock
$\tau$	Scaling factor	-	$\tau = e^2$
$D_w$	Damkohler Coefficient	m <sup>2</sup> /s	$D_w = \frac{L\phi R_n}{C_{eq}}$
$T_f$	Residence time	$10^{-6}$ s	$T_f = \frac{L\phi}{q}$
$C_{eq}$	Equilibrium concentration	μmol/L	Max Catchment
$C_0$	Initial concentration	μmol/L	Rain Conc

Table 3: Key parameters and definitions for the Maher model.

### 5.3.3 Comparison of the Models

<b>Fontorbe</b>	<b>Maher</b>
$T_f = \frac{(C_h - C_o) \cdot \phi}{(1 - f) \cdot R_n}$	$T_f = \frac{C_{eq} \cdot (C - C_0)}{e^2 R_n (C_{eq} - C)}$
$R_n = \frac{(C_h - C_o) \cdot \phi}{(1 - f) \cdot T_f}$	$R_n = \frac{C_{eq} \cdot (C - C_0)}{e^2 T_f (C_{eq} - C)}$

Table 4: Comparison of equations from Fontorbe and Maher

From this table comparison, it is easy to see the differences between why the two models will differ in their estimation of residence time.

For residence time, both contain the factor - but the RN IS DEFINED DIFFERENTLY TOO

$$\frac{C - C_o}{R_n}$$

The difference then comes with the remaining variables in the reaction. For Fontorbe, the porosity divided by the fraction of element reprecipitated makes up the remaining terms. For Maher, the equilibrium concentration divided by the scaling factor and the difference between the equilibrium concentration and the concentration of the element make up the remaining terms.

Given that both the fraction of element reprecipitated and the scaling factor range between 0-1, the difference in the models will come from the equilibrium concentration in the Maher formula. Indeed, given that the concentration is taken from the highest in the catchment (so as not to follow Maher and Chamberlain (2013)'s rather conservative estimate following Gaillardet et al. (1999)'s global river data), the fraction

$$\frac{C_{eq}}{C_{eq} - C}$$

will only get larger as the reaction progresses. As the reaction progresses, the Maher model will predict longer times than the Fontorbe model, in the end with two orders of magnitude difference at the older times.

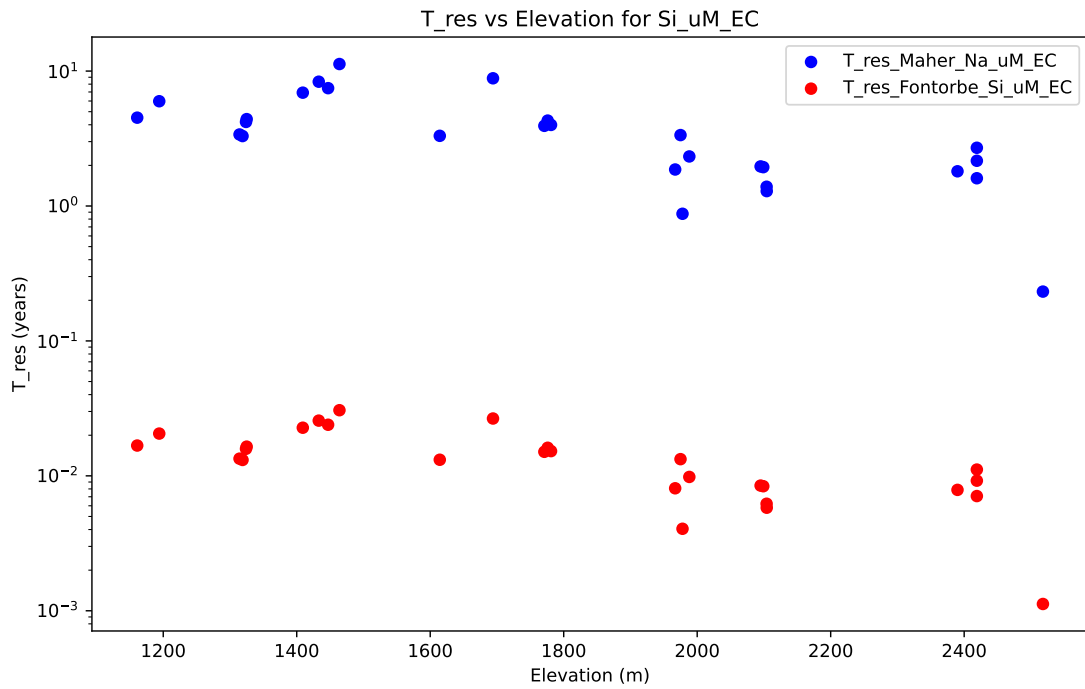


Figure 20: Comparison for the residence time between the two models. Evaluated for Specific surface area = 0.1; Mineral concentration in rock = 0.36; density of plagioclase = 2.230; Reaction rate constant = 10-15; Porosity = 0.3; Equilibrium concentration = Max in the catchment = 900 uM; Initial concentration = smallest in the traverse; Fraction reprecipitated = 0.5.

### 5.3.4 Constraints on Residence Time

As per Acharya et al. (2020), parts of the literature suggest that the most amount of precipitation occur in the top quarter of the Himalayan catchments. Studies analysing gas ages suggest that the residence time of the water in this catchment is on the order of 10 years, with an average of 25 years (Atwood et al, 2020).

Assuming an average rainfall rate of 3.5 m/yr (cite) over the top quarter of the catchment which is approximately 1km long, a m<sup>2</sup>/yr rate of 3500 is obtained. When considering a 10m wide channel

flow of water, a flow rate of 350 m/yr for the top quarter of the catchment is obtained.

Secondly, using the oxygen isotopic composition of the springs, and comparing to the rainfall line, it is possible to obtain a flow path length assuming a general slope of 20 degrees:

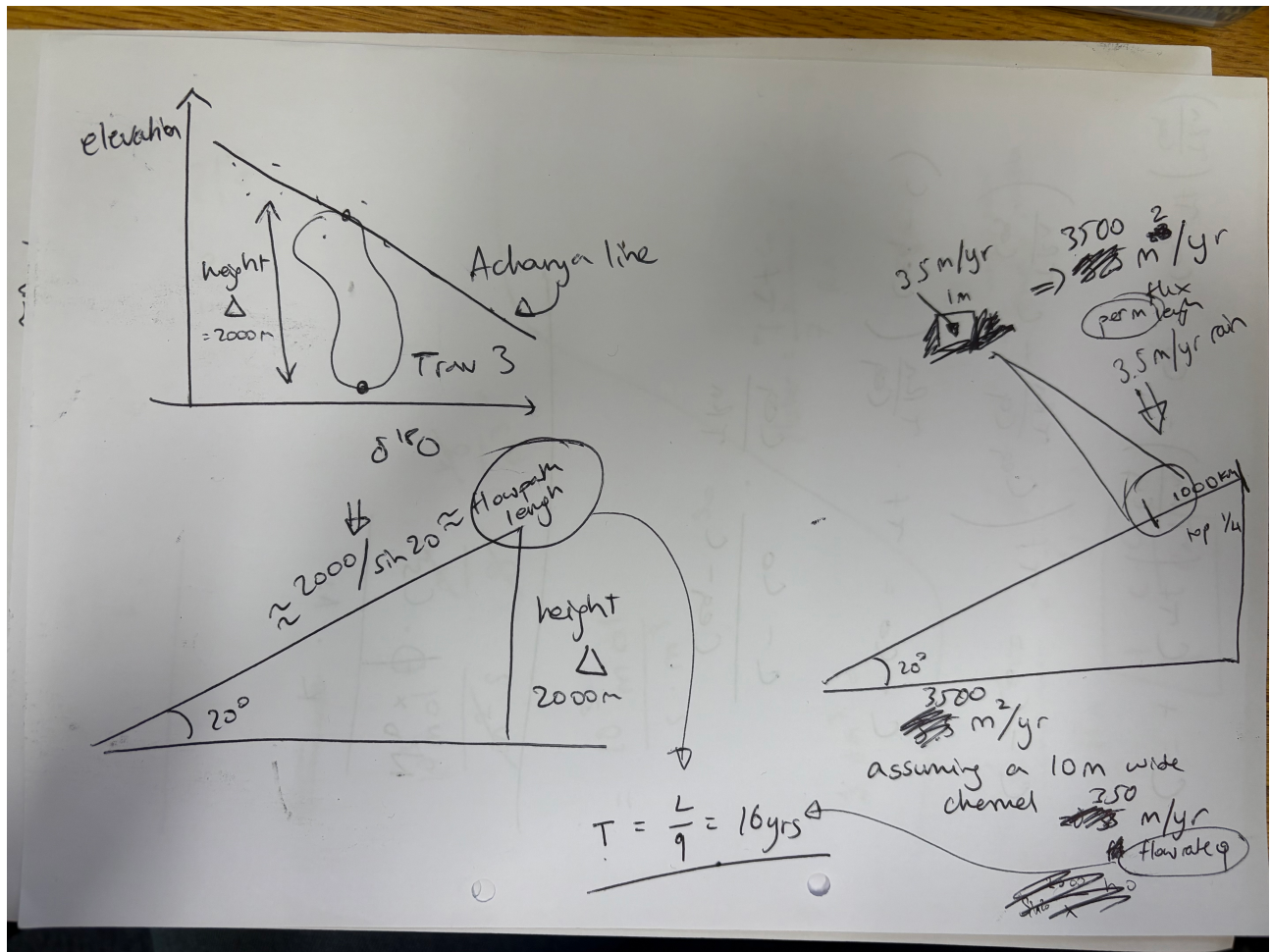


Figure 21: Proving the point that residence time is around 10 years

In this way it is plausible that 10 years could be how long the water is spending in the catchment, consistent with the Maher model.

## 5.4 Free Energy Calculations

- Delta G can be calculated from the saturation index of the minerals from PhreeQC
- Because of the solid solution of feldspar, we have a lowering of delta G as per Dubacq
- Compare Delta G against the times obtained from the Maher model. Is Maher correct?

### 5.4.1 Comparison with Residence Time

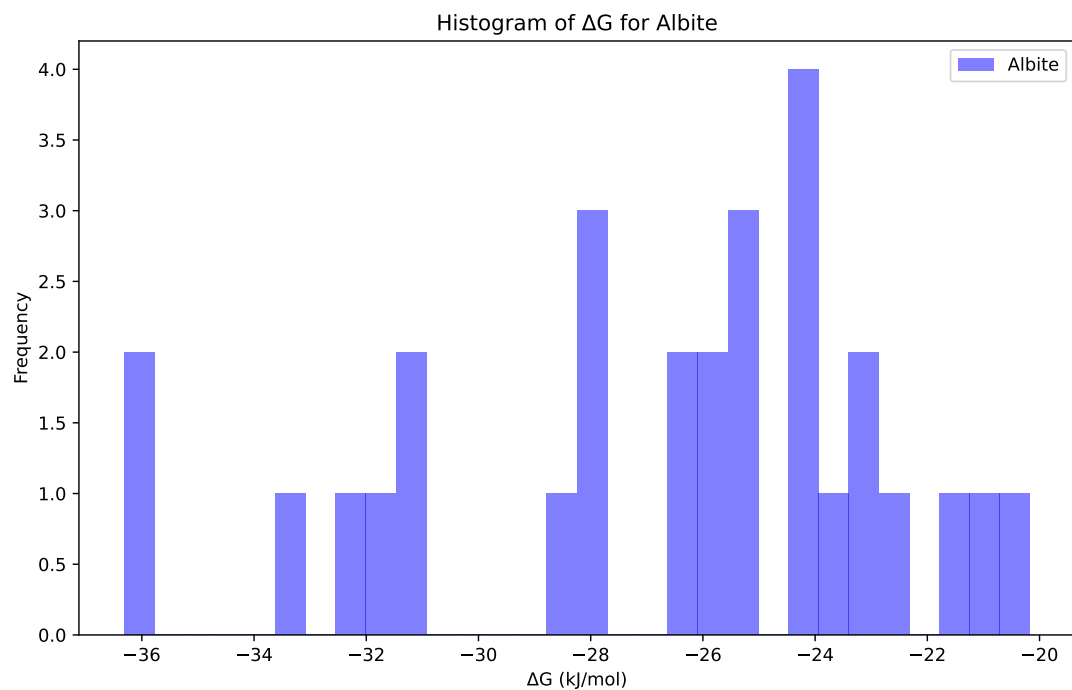


Figure 22: Histogram of the delta G of albite

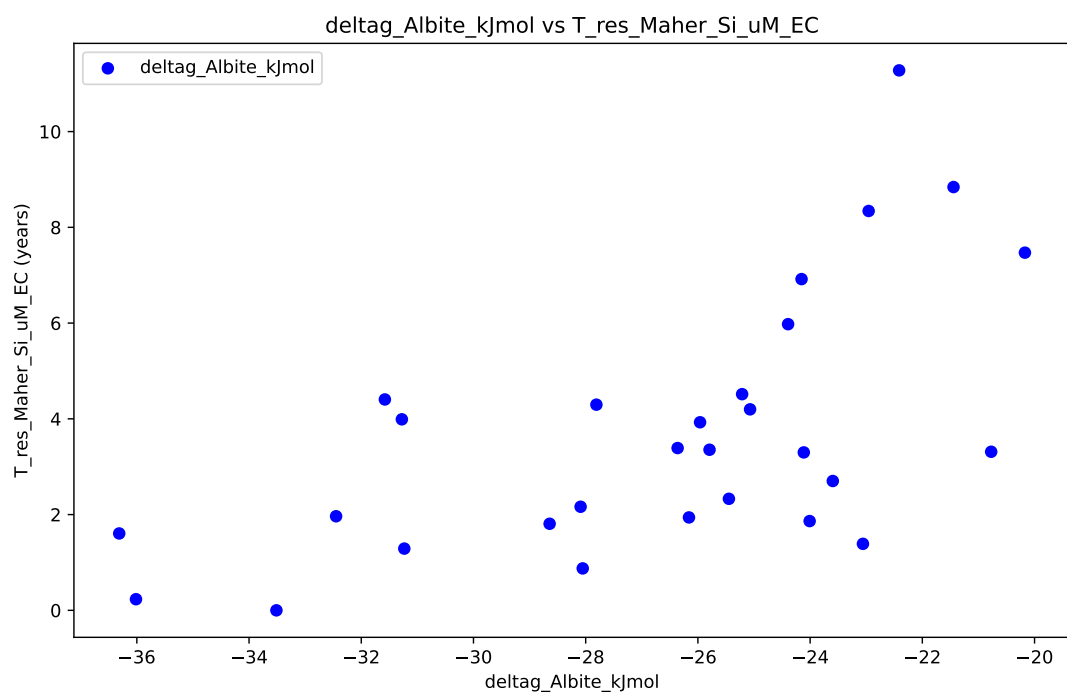


Figure 23: Comparison of the delta G of albite against the residence time from the Maher model.

### 5.4.2 Constraints on Reaction Rate

If a residence time of 10 years is appropriate, the models can be used to determine the reaction rate. This can then be used to determine whether weathering is sensitive to the fluid flux moreso than it is to the temperature, and that the water particles are close to equilibrium when comparing to the distance from equilibrium.

With a residence time of 10 years, it is possible to see what the reaction rate is using the following relationship:

$$R_n = \frac{C_{eq} \cdot (C - C_0)}{e^2 T_f (C_{eq} - C)} \quad (27)$$

$$\rho_{sf} \cdot k \cdot A \cdot X_r = \frac{C_{eq} \cdot (C - C_0)}{e^2 T_f (C_{eq} - C)} \quad (28)$$

$$k = \frac{C_{eq} \cdot (C - C_0)}{e^2 T_f (C_{eq} - C) \cdot \rho_{sf} \cdot A \cdot X_r} \quad (29)$$

Taking the range of samples that correspond to MKS-5 to MKS-9, the places where Atwood et al, 2020 took their lowest elevation sample and found a time of 13 years, we can calculate the reaction rate constant, and compare it to the delta g assuming a simple increase in time with the samples. Note that the time Atwood found for their samples did not ascribe to this simple linear decrease, nor do we expect the time to do so. But for a proof of concept it should demonstrate how the rates of reaction plot:

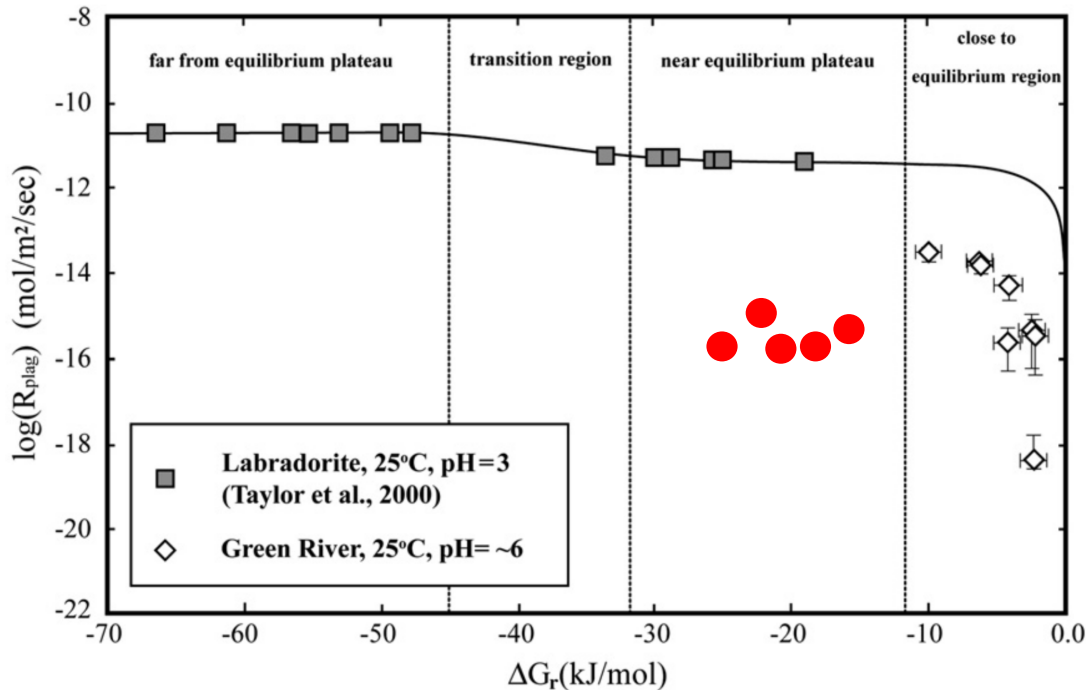


Figure 24: Proving the point that the reaction rate is 10-15.

It is clear from this plot that the obtained reaction rate is of the order of  $10^{-15}$  mol/m<sup>2</sup>/s. However unlike it does not show a decrease that we would expect if the system was truly approaching equilibrium. Indeed the delta G is still in Kampman's "near equilibrium plateau". And there is still a ways to go before the system is truly close to equilibrium. Insert sentence about obviously Kampman is a different system but the point is that the system is not close to equilibrium.

So Maher's model for this natural system is not apt in showcasing that

## **References**

## 6 Appendix 1: Dimensional Analysis of $T_f$

### Fontorbe Model

The residence time  $T_f$  is given by:

$$T_f = \frac{(C_h - C_0) \cdot \phi}{(1 - f) \cdot R_n} \quad (30)$$

where the parameters have the following units:

- $C_h, C_0$  (Concentration):  $\mu\text{mol/L}$

$$1 \mu\text{mol/L} = \frac{10^{-6} \text{ mol}}{10^{-3} \text{ m}^3} = 10^{-3} \frac{\text{mol}}{\text{m}^3}$$

- $\phi$  (Porosity) is dimensionless.
- $f$  (Fraction reprecipitated) is dimensionless.
- $R_n$  (Reaction rate) is given by:

$$R_n = k \cdot S \cdot \rho \cdot 10^3 \cdot X \cdot (1 - \phi) \quad (31)$$

where:

- $k$  (Reaction rate constant):  $\left[ \frac{\text{mol}}{\text{m}^2 \cdot \text{s}} \right]$
- $S$  (Specific surface area):  $\left[ \frac{\text{m}^2}{\text{g}} \right]$
- $\rho$  (Mineral density):  $\left[ \frac{\text{kg}}{\text{m}^3} \right]$

Since  $1 \text{ kg} = 10^3 \text{ g}$ , we write:

$$\rho = \frac{10^3 \text{ g}}{\text{m}^3}$$

- $X$  (Volume fraction of mineral in rock) is dimensionless.
- $(1 - \phi)$  is dimensionless.

### Step-by-Step Dimensional Analysis of $R_n$

First, multiplying  $k$  and  $S$ :

$$k \cdot S = \left( \frac{\text{mol}}{\text{m}^2 \cdot \text{s}} \right) \times \left( \frac{\text{m}^2}{\text{g}} \right) = \frac{\text{mol}}{\text{g} \cdot \text{s}}$$

Next, multiplying by  $\rho$ :

$$\left( \frac{\text{mol}}{\text{g} \cdot \text{s}} \right) \times \left( \frac{10^3 \text{ g}}{\text{m}^3} \right) = \frac{10^3 \text{ mol}}{\text{m}^3 \cdot \text{s}}$$

Since  $X$  and  $(1 - \phi)$  are dimensionless, they do not affect the units.

Thus, the final unit of  $R_n$  is:

$$R_n = \frac{10^3 \text{mol}}{\text{m}^3 \cdot \text{s}}$$

### Final Dimensional Analysis of $T_f$

Substituting the units:

$$T_f = \frac{(C_h - C_0) \cdot \phi}{(1 - f) \cdot R_n}$$

Since  $C_h - C_0$  has units of:

$$10^{-3} \frac{\text{mol}}{\text{m}^3}$$

and  $R_n$  has units of:

$$\frac{10^3 \text{mol}}{\text{m}^3 \cdot \text{s}},$$

we get:

$$T_f = \frac{10^{-3} \frac{\text{mol}}{\text{m}^3}}{10^3 \frac{\text{mol}}{\text{m}^3 \cdot \text{s}}}$$

Canceling  $\frac{\text{mol}}{\text{m}^3}$ :

$$T_f = \frac{10^{-3}}{10^3} \cdot s = 10^{-6} s$$

### Conclusion

The predicted unit of  $T_f$  is:

$$T_f \sim 10^{-6} \text{s}$$

## Maher Model

### Given Equation for $T_f$

The residence time  $T_f$  is given by:

$$T_f = \frac{C_{eq} \cdot (C - C_0)}{e^2 R_n (C_{eq} - C)} \quad (32)$$

where the parameters have the following units:

- $C_0, C, C_{eq}$  (Concentrations) in  $\mu\text{mol/L}$ :

$$1 \mu\text{mol/L} = 10^{-6} \frac{\text{mol}}{\text{L}}$$

Thus,

$$C_0, C, C_{eq} \sim 10^{-6} \frac{\text{mol}}{\text{L}}$$

- $R_n$  (Net reaction rate) is defined as:

$$R_n = \rho_{sf} \cdot k \cdot A \cdot X_r$$

where:

- $\rho_{sf}$  (Mass mineral/Fluid Volume ratio) has units:

$$\rho_{sf} \sim \frac{\text{g}}{\text{L}}$$

- $k$  (Reaction rate constant):

$$k \sim \frac{\text{mol}}{\text{m}^2 \cdot \text{s}}$$

- $A$  (Specific surface area):

$$A \sim \frac{\text{m}^2}{\text{g}}$$

- $X_r$  (Mineral concentration in fresh rock) is dimensionless.

### Step-by-Step Dimensional Analysis of $R_n$

Expanding  $R_n$ :

$$R_n = \left( \frac{\text{g}}{\text{L}} \right) \times \left( \frac{\text{mol}}{\text{m}^2 \cdot \text{s}} \right) \times \left( \frac{\text{m}^2}{\text{g}} \right)$$

Canceling g and  $\text{m}^2$ :

$$R_n = \frac{\text{mol}}{\text{L} \cdot \text{s}}$$

Thus, the reaction rate  $R_n$  has the units:

$$R_n \sim \frac{\text{mol}}{\text{L} \cdot \text{s}}$$

### Dimensional Analysis of $T_f$

Substituting the units into:

$$T_f = \frac{C_{eq} \cdot (C - C_0)}{e^2 R_n (C_{eq} - C)} \quad (33)$$

- \*\*Numerator:\*\*

$$C_{eq} \cdot (C - C_0) \sim 10^{-12} \frac{\text{mol}^2}{\text{L}^2}$$

- \*\*Denominator:\*\*

$$e^2 R_n (C_{eq} - C)$$

Since  $e^2$  is \*\*dimensionless\*\*, we are left with:

$$e^2 R_n \sim 10^{-6} \frac{\text{mol}^2}{\text{L}^2 \cdot \text{s}}$$

Now, dividing:

$$T_f = \frac{10^{-12} \frac{\text{mol}^2}{\text{L}^2}}{\frac{10^{-6} \text{mol}^2}{\text{L}^2 \cdot \text{s}}}$$

Canceling  $\frac{\text{mol}^2}{\text{L}^2}$ :

$$T_f = 10^{-6} \text{s}$$

### Conclusion

The predicted unit of  $T_f$  is:

$$T_f \sim 10^{-6} \text{s}$$

which corresponds to:

$$T_f = 1 \mu\text{s} \quad (\text{microseconds}).$$

**Remember to add a box explaining Sr isotopes in the Appendix**

Hello